Perfluorosulfonated Ionomers Membranes: Melt-Processing and Characterization for Ion Exchange Applications

Weihua Tang,[1] Rui Zhang,[2] Beibei Liu,[1] Huilin Yuan[2]

[1]Key Laboratory of Soft Chemistry and Functional Materials, Ministry of Education, Nanjing University of Science and Technology, Nanjing 210094, People's Republic of China

[2]Key Laboratory of Beijing City on Preparation and Processing of Novel Polymer Materials, Beijing University of Chemical Technology, Beijing 100029, People's Republic of China

Correspondence to: W. H. Tang (E-mail: whtang@mail.njust.edu.cn) or H. L. Yuan (E-mail: yuanhuil@263.net)

ABSTRACT: Perflurosulfonated ionomers membranes with different ionic-exchange capacity were successfully fabricated via melt-extruding and casting of their $-SO_2F$ precursors. A systematical investigation of the thermal stability, crystallinity, and rheological properties of the precursors was performed to secure their optimized processing conditions. The tensile properties of acid-form membranes are found to increase with base-hydrolysis time, where a tensile strength of 38.2 MPa is readily obtained after 24 h's base-hydrolysis. The content of $-SO_2F$ or $-SO_3H$ containing side-chains plays an important role in the thermal stability, rheological, and mechanical properties of the precursor or the acid-form membranes. The strong ionic interactions, attributed to the $-SO_3H$ groups, lead to decreased crystallinity and tensile strength for different IEC membranes. The acid-form membranes exhibit good proton conductivity and low methanol crossover in comparison with reference Nafion membrane. © 2013 Wiley Periodicals, Inc. J. Appl. Polym. Sci. **2014**, *131*, 39944.
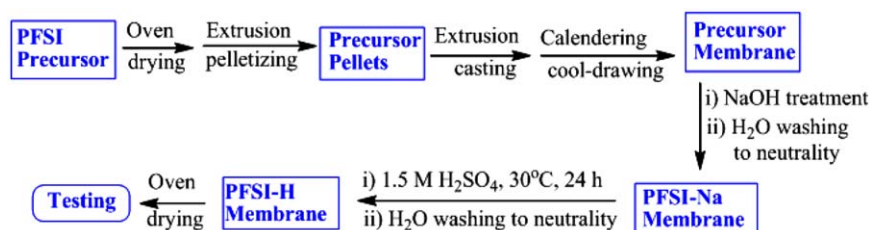
INTRODUCTION

Perfluorosulfonated ionomers (PFSI), featuring excellent electro-chemical and mechanical properties, have been successfully used in membranes for electrolysis industry and proton-exchange membrane fuel cells.[1–3] PFSI are typically synthesized by copoly-merization of tetrafluoroethylene and perfluorovinylether, and thus their polytetrafluorothylene (PTFE) backbone is grafted with active sulfonate-containing side-chains for ion-exchange purpose.[1] The length of the side-chain plays a crucial role in the properties of the final membranes. For this reason, numerous literatures have reported the properties and applications of conventional ionomers including so-called Long-Side-Chain (LSC) monomers such as Nafion® (Dupont),[1] Flemion® (Asahi glass), and Aciplex® (Asahi Kasei),[4] and Short-Side-Chain (SSC) monomer like Aquivion® (Solvay Specialty Polymers).[5] Perfluorosulfonated ionomers are usually derived from their thermoplastic sulfonyl fluoride ($-SO_2F$) precursors. Free of strong interactions between ionic groups to form clustered morphology, the $-SO_2F$ precursors can be readily extruded into sheets of required thickness.[1] PFSI membranes were then activated via base-hydrolysis to achieve the salt form or further acid-hydrothermal to obtain $-SO_3H$ form for practical applications.

The membranes are commonly characterized by their thickness, ion exchange capacity (IEC, mmol SO_3H/g polymer) or equivalent weight [EW (g/mol) = 1000/IEC].

A great number of articles have reported the concerted efforts in research and development of solution-cast PFSI membranes since the first processing procedure developed by Moore and Martin in 1986.[6] Solution-casting was facile to prepare coatings on modified electrodes,[1] permselective membranes for desalination,[7] films for fuel cells,[6,8,9] and recast membranes[10] with excellent mechanical properties. But the good mechanical properties of the cast membranes are strongly dependent on the solvent system and annealing treatment used for casting. To achieve flexible and solvent-resistant membranes, PFSI membranes generally have to be cast at high temperature (over 200°C) from polar solutions of high boiling points.[6] It is, however, challenging to achieve good solution-cast membranes with the similar properties and solubility as the as-received Nafion® membranes. DMF is proved to be a good solvent to prepare solution-casting PFSI membranes.[3,10] Study has shown that only the re-cast Nafion® 112 membranes from DMF-dispersion gave the conductivity performance comparable to those of commercial membranes.[11] The basic homogeneous membranes can also be

Scheme 1. The synthesis of perfluorosulfonated precursors and the chemical structures of PFSI ($m = 3$–8) and Nafion®.[3]

modified to meet specific applications. Examples like introducing weave fabric,[12,13] porous PTFE films,[14] or inorganic particles[15,16] to fabricate composite membranes to achieve improved mechanical properties, permselectivity and /or fuel cell performance.

Recently, Dongyue Research Institute in China has developed a series of PFSI precursors, structurally similar to the ionomers reported by Sauguet et al.[17] In Scheme 1, the radical copolymerization of tetrafluoroethylene and perfluoro[2-(2-fluorosulfonylethoxy) propyl vinyl ether] the copolymerization was initiated using perfluoroacyl peroxide in fluorocarbon solvent. After conversion of $-SO_2F$ groups into $-SO_3Na$ or $-SO_3H$, the PFSI membranes are proved to be a good alternative to Nafion® in most applications. In Scheme 1, the perfluorosulfonated ionomers (PFSI) developed by Dongyue Research Institute are structurally different with Nafion® in terms of backbone. For these new precursors, solution-casting membranes can be readily prepared with the techniques of Nafion®.

Inspired by our research experience in melt-extrusion of polymer composites and calendaring films for various engineering applications,[18–21] we are intrigued with the fabrication of PFSI membranes via melt-extrusion and their further reinforcement via direct calendaring processing. In this article, we report herein our research effort in the development of extrusion-casting PFSI membranes. PFSI precursors were carefully studied in terms of thermal stability, rheological properties, and crystallinity to obtain their processing properties for melt-extrusion and casting of precursor membranes. By extrusion-casting of precursor membranes with the optimized processing temperatures, the acid form PFSI membranes were obtained with base-hydrolysis and acid-hydrothermal processing. The structure, crystallinity, and tensile properties of the acid-form PFSI membranes were studied in detail. This study may provide a good guidance on the melt-processing of different IEC PFSI membranes with high mechanical properties for applications.

EXPERIMENTAL

Materials
Perfluorosulfonated ionomer precursors were provided by Dongyue Research Institute (Shandong, China). In Scheme 1, they are synthesized via radical copolymerization of tetrafluoroethylene

and perfluoro[2-(2-fluorosulfonylethoxy) propyl vinyl ether] in the presence of perfluoroacyl peroxide in fluorocarbon solvent. After copolymerization, the precursor with sulfuryl fluoride functional groups was separated, rinsed, dried, and granulated in a twin-screw extruder. By varying the ratio of monomers, PFSI precursors with different IEC values can be prepared. For a comparison with Nafion 117, three PFSI precursors with close IEC values were selected as model resins in this study. They have a density of 1.98 g/cm^3. Nafion 117 membranes (IEC 0.91) from DuPont were pretreated subsequently with 2% H_2O_2, deionized water and 0.5M H_2SO_4 aqueous solution according to the procedure in Ref. 3 and stored in water until required.

Preparation of PFSI Membranes
The PFSI precursors were dried at 80°C in a constant temperature oven for 12 h. The massive resins were pelletized by melt-extrusion, where a single-screw Brabender PLD-651 extruder (Germany, Φ30, L/D = 25) was used and the compression ratio of the screw was fixed at 3 : 1. The PFSI casting membranes (0.25 mm in thickness) were further prepared by extrusion from a co-extrusion casting die with a slit (200 × 1.5 mm) and calendared with a three-roll calendar (U120 200; Brabender, Germany) on the same above-mentioned extruder. The clear and transparent precursor membranes were obtained after direct cooling from calendaring process.

The as-prepared PFSI membranes were first converted to their sodium salt form (PFSI-Na) by immersing in 20% sodium hydroxide at 80°C for 24 h (unless specified), followed by washing with deionized water till pH 7 (Scheme 2). The PFSI-Na membranes were further converted into the required acid form (PFSI-H) by immersing in 1.5M sulfuric acid solution at 30°C for 24 h, followed by immersion in deionized water for 24 h. The deionized water was changed every 6 h in an effort to remove all of the residual sulfuric acid in the membrane. The membranes were finally dried overnight in oven at 80°C before testing.

IEC Measurement
The ion exchange capacity of PFSI-H membranes was determined using acid–base titration method. The membranes were soaked in 1M NaCl solution for 24 h to exchange sodium cation

Scheme 2. Flowchart of the fabrication of PFSI membranes via extrusion casting and calendaring. [Color figure can be viewed in the online issue, which is available at wileyonlinelibrary.com.]

for the protons. The membranes were taken out and soaked in a fresh $1M$ NaCl solution for another 24 h. The solutions from two ion-exchange processes were combined and titrated with $0.1M$ NaOH using pH-metry method. For each membrane, at least three replicates were performed with average value reported as the IEC. The IEC of three membranes was determined to be 0.92, 0.97, and 1.05 mmol/g, respectively. The corresponding equivalent weight (EW) of these membranes was accordingly calculated to be 1087, 1031, and 952 g/mol. For simplicity in description, the PFSI precursor corresponding to membrane of certain IEC value was denoted as IEC_n, where the n (without the unit of mmol/g) is the IEC value of the membrane. The PFSI precursors were denoted as IEC0.92, IEC0.97, and IEC1.05, respectively.

Thermal and Optical Properties

Thermal gravimetric analysis (TGA) was recorded on Perkin-nElmer TG S-2 (PerkinElmer, UK) under N_2 atmosphere in the temperature range of 25–750°C with a heating rate of 20°C/min. The phase composition of casting PFSI-H membranes was characterized by D/Max2500VB2+/PC XRD diffractometer (Rigaku, Japan) with a 2θ ranging between 3° and 60°. About 5 μm thick IEC0.92 and PFSI-H membranes were examined by ATR-IR in a Nicolet 205 spectrometer with attenuated total reflectance (ATR) technique. A KRS-5 (thallium bromoiodide) crystal was used. ATR-IR spectra were recorded from 4000 to 500 cm^{-1} with an incidence angle of 45°. Altogether 200 scans were averaged for every spectrum with 4 cm^{-1} resolution.

Rheological Properties Measurements

The MFI values of PFSI precursors (pre-dried at 80°C for 12 h) were determined on XNR-400 analyzer (Chengde, China) at specified temperature under the load of 21.6 N. The apparent viscosities of PFSI precursors at various shear rates were measured using an Instron 3211 capillary rheometer. The capillary diameter was 1.2 mm and the L/D ratio was 42.58. The experiments were carried out at 190, 200, and 210°C under shear rate ranging between 1 and 10^4 s^{-1}. The mixing torque of PFSI precursors was measured with a HAAKE Polylab OS (Thermo-Electron, Germany) with a mixer volume of 49 mL at temperature ranging between 190 and 240°C for 15 min, and the rotational speed was set as 50 rpm. The torque was recorded as a function of time.

Mechanical Properties Measurements

The tensile strength of PFSI membranes was measured on an Instron 1185 universal tester as per GB13022-91 method. The crosshead speed was set as 10 mm/min for tensile tests at 20°C

and 50% humidity. The value was calculated as average over six to eight specimens for each membrane.

Water Uptake Measurements

Water uptake of the fully hydrated PFSI-H membranes was measured by boiling the membrane samples in 3 wt % hydrogen peroxide, deionized water, and $2M$ sulfuric acid for 1 h, respectively. The membranes were then taken out, wiped and weighted to obtain the wet weight (W_w). The membranes were then dried over 80°C for 24 h to get their dry weight (W_d). The water uptake was calculated as $[(W_w - W_d)/W_d] \times 100\%$, where the average value of five samples was counted.

Proton Conductivity Measurements

The in-plane proton conductivity of the membranes was carried out using a four probe method at 25°C in deionized water. The proton conductivity was calculated using equation $\sigma = L/RA$, where L is the distance between the electrodes, A is the cross-sectional area of the membrane, and R is the resistance of the membrane. The thickness of the membranes was determined using a digital micrometer. At least four samples of each membrane were evaluated to determine the proton conductivity.

RESULTS AND DISCUSSION

Thermal Stability of PFSI Precursors

The thermal stability of PFSI precursors is one of the key issues in developing extrusion-casting PFSI membranes. As TGA curves shown in Figure 1(a), the PFSI precursors, i.e., IEC0.92, IE0.97, and IEC1.05 exhibited excellent thermal stability, with negligible weight loss observed below 400°C. The decomposition temperatures (5% weight loss) of all three precursors are higher than 450°C (inset table). However, the precursors differ in their thermal stability relative to the content of –SO$_2$F containing side-chains. The precursor with higher content of such side-chains exhibits larger weight loss when subjected to heating. This is easy to understand since the first stage of thermal decomposition of PFSI precursor occurs due to the cleavage of –SO$_2$F from the perfluorovinylether side-chains.

In order to reveal the thermal stability of PFSI precursors for repeatable melt processes, special TGA measurements with continuous heating–cooling cycles were conducted. In Figure 1(b), the precursor of IEC0.97 membrane was continuously heated up to 300°C within 11 heating–cooling cycles, where the heating temperature gradually increased by 10°C interval per-cycle starting from 200°C. The results show the precursor possesses excellent thermal stability even when subjected to repeated heating–cooling cycles. The weight loss less than 0.1% is observed during
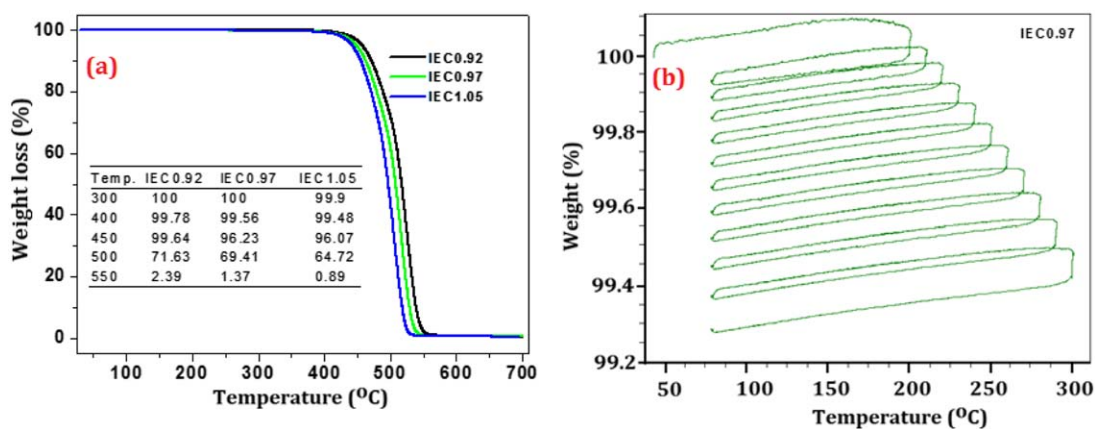
Figure 1. (a) TGA curves of three PFSI precursors in temperature ranging between 25 and 700°C, and (b) TGA curve of IEC0.97 precursor within 11 heating–cooling cycles, where heating temperature gradually increased by 10°C interval from 200 to 300°C. [Color figure can be viewed in the online issue, which is available at wileyonlinelibrary.com.]

very heating–cooling cycle in the whole TGA measurement, indicating the PFSI precursor is well suited for the melt-extrusion process for mass-production of large-scale membranes.

Crystallinity Measurement

The crystallinity of three PFSI precursors was compared using XRD study. In Figure 2, all membranes show a distinct peak centered at $2\theta \approx 17°$, which can be attributed to the diffraction maxima of PTFE regions. This peak can be further deconvoluted into two peaks, one abroad scattering peak at $2\theta \approx 15.5°$ and another sharp peak at $2\theta \approx 17.5°$. The broad peak is corresponding to the diffraction maxima of amorphous phase, while the sharp peak is assigned to the crystalline scattering from the polyfluorocarbon backbone, respectively.[22,23] In agreement with the previous studies, the Bragg spacing (0.5075 nm) calculated for $2\theta \approx 17.5°$ is very close to the interplanar spacing of PTFE (0.4987 nm).[23]
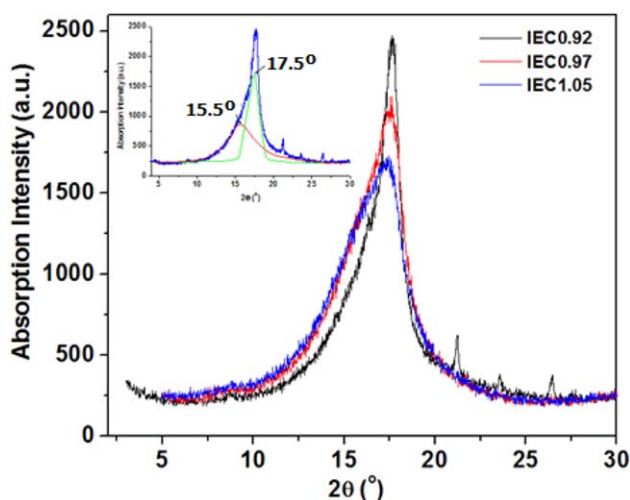
Figure 2. XRD curves of three PFSI precursor membranes. Inset figure illustrates the deconvolution of the XRD curve of IEC0.92 to fitted curves for amorphous region (at $2\theta \approx 15.5°$) and for crystalline peak (at $2\theta \approx 17.5°$), respectively. [Color figure can be viewed in the online issue, which is available at wileyonlinelibrary.com.]

The crystallinity of PFSI precursors can be roughly compared with the deconvoluted peaks centered at ~17.5° and ~15.5°.[10] In Figure 2, the intensity of diffraction peaks of three PFSI precursors decreases in the order of IEC0.92, IEC0.97 and IEC1.05. However, the full-width at half maximum (FWHM) for the deconvoluted peak ($2\theta \approx 15.5°$) increases with the increasing content of $-SO_2F$ containing side-chains, indicating the greater portion of amorphous phase of perfluorocarbon (PTFE) chains in the membranes. It is, thus, evident that the crystallinity of three precursors decreases in the order of the increasing content of $-SO_2F$ containing side-chains.

The decrease in crystallinity with increasing content of $-SO_2F$ containing side-chains can be explained with the structure difference of the PFSI precursors. As mentioned earlier, PFSI precursors feature a polymer structure with polyfluorocarbon backbone and perfluoro[2-(2-fluorosulfonylethoxy) propyl vinyl ether] side-chains ending with $-SO_2F$ group. The polyfluorocarbon backbone is semicrystalline as PTFE. With increasing the content of $-SO_2F$ containing side-chains, the total crystallinity of the resulted precursors decrease due to the increased steric hindrance of side-chains, resulting in a much slower and more incomplete rearrangement of polymer chain into ordered structure.

Melt Flow Index Test

Melt flow index (MFI) is a useful parameter to describe the flowing properties of thermoplastic melt like PFSI precursors. The variation of MFIs of three PFSI precursors with melt temperature is depicted in Figure 3, where the melt of specific temperature flows through a channel with regular diameter and length as per ASTM D1238. As shown, the PFSI precursors exhibit increased MFI values at higher melt temperature, with a highest MFI of 16.2, 20.3, and 19.2 g/10 min achieved at 220, 240, C and 260°C, respectively, for IEC0.92, IEC0.97, and IEC1.05. It is noted that PFSI precursors for lower IEC membranes exhibits lower melting temperature. Three precursors present a melting point of 160, 180, and 200°C, respectively. This phenomenon is in good agreement with the crystallinity
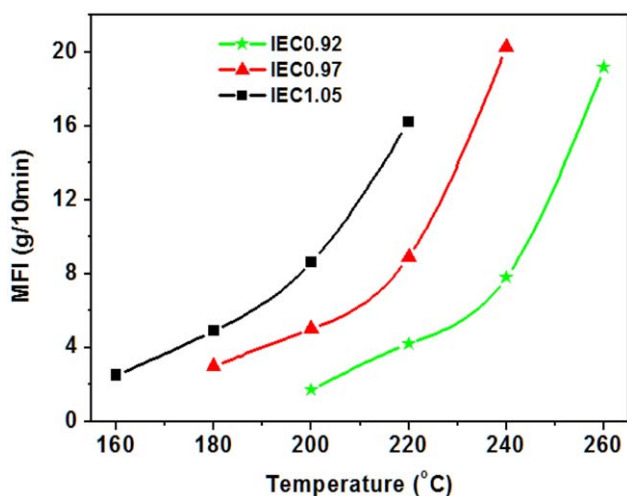
Figure 3. The MFI values of three PFSI precursors at different melt temperatures. [Color figure can be viewed in the online issue, which is available at wileyonlinelibrary.com.]

study above, i.e., higher melting energy is required for PFSI precursors with higher –SO_2F containing side-chains.

Empirically, thermoplastics with a MFI of 3–5 g/10 min are good for extrusion-casting processing, while those with a MFI of 6–10 g/10 min are better to be processed via molding-casting in membrane fabrication.[24] Therefore, the best processing temperature range for three PFSI precursors is 180–187°C for IEC0.92, 195–203°C for IEC0.97 and 227–235°C for IEC1.05, respectively.

Capillary Rheological Study

The rheological property of polymers/blends is very important in optimizing their melt-processing conditions.[25] The flow behavior of polymer melt under shearing when extruded out from a capillary can be a guidance for setting processing parameters such as melt-extrusion temperature, heating time, and screw speed for extrusion-casting of PFSI precursor membranes.

As known to all, most polymer melts are non-Newtonian fluids, whose apparent viscosity varies with shear rate in accordance to the equation[26]:

$$\eta = k \, \gamma^{\,n-1} \tag{1}$$

After taking logarithm, eq. (1) can be expressed as

$$\log \, \eta = \log k + (n-1)\log \, \gamma \tag{2}$$

where η is the apparent viscosity (Pa·s), γ the shear rates (s^{-1}), n the non-Newtonian index and k a constant. The non-Newtonian index can thus be obtained by the slope of the straight line when plotting log η against log γ.

The apparent viscosity of IEC0.92 precursor was measured at 190C, 200, and 210°C [Figure 4(a)]. It is found that the PFSI precursor exhibits a relatively low viscosity. And the viscosity decreases with the shear rate, a typical shear-thinning behavior as most non-Newtonian fluids. Importantly, the apparent viscosity is found to decrease with temperature at same shear rate. Such phenomenon could be explained by the entanglement of the polymer segments. During the flow of a polymer melt, the molecular chains are disentangled by shear and re-entangled by thermo-motion. If the rate of the former is less than the latter, the viscosity is low. At higher temperatures, polymer melt may have larger free volume for the movement of polymer chains/segments, thus leading to lower entanglement of polymer chain.

The apparent viscosity of PFSI precursors decreases with the increment of –SO_2F containing side-chains when compared the curves of log η versus log γ for IEC0.92 and IEC0.97 precursors, as shown in Figure 4(b). This behavior can be explained with the crystallinity of PFSI precursors. As know, PFSI precursors with higher side-chain content (ca. IEC0.97) display lower crystallinity and thus less re-entanglement of polymer chains at the melt state. When the molecular chains are disentangled by shear, IEC0.97 will present much lower viscosity for the melt.

By extracting the slope of the plot of log η versus log γ, the non-Newtonian index can be obtained for PFSI precursors at specific temperature. As summarized in Table I, the non-Newtonian index is found to increase with melt temperature, indicating that the increasing of processing temperature can facilitate the melting of PFSI precursors and reduce their melt viscoelasticity for more efficient extrusion. PFSI precursors exhibit better melt processability when more side-chains are
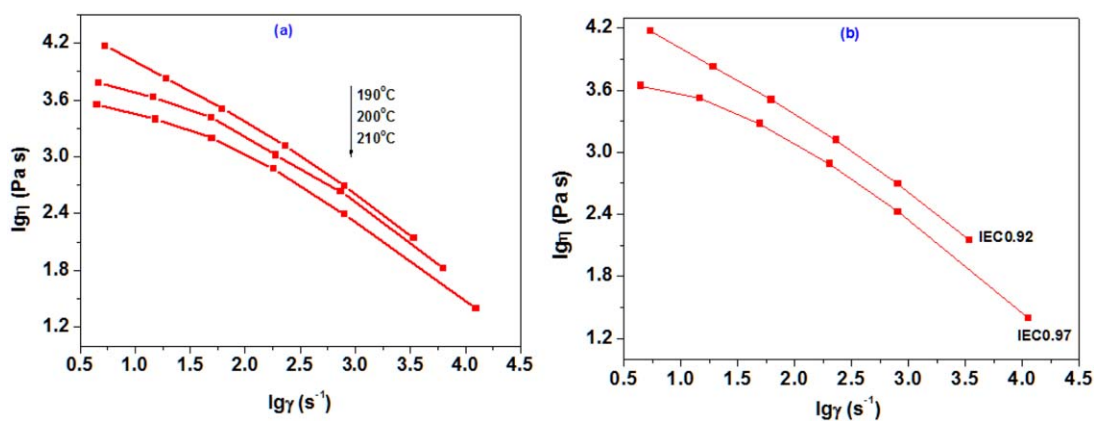

Figure 4. Plot of apparent viscosity versus non-Newtonian shear rate of (a) IEC0.92 at temperature ranging from 190 to 210°C, and (b) IEC0.92 and IEC0.97 at 190°C. [Color figure can be viewed in the online issue, which is available at wileyonlinelibrary.com.]

Table I. Temperature-Dependant Non-Newtonian Index for PFSI Precursors

Precursors	130°C	140°C	150°C	190°C	200°C	210°C
IEC0.92	–	–	–	0.34	0.58	0.61
IEC0.97	–	–	–	0.49	0.60	0.63
IEC1.05	0.56	0.63	0.66	–	–	–

(–) Not available.

contained, e.g., IEC1.05 shows even higher n at temperature (ca. 140 and 150°C) than IEC0.92 and IEC0.97 at higher temperature (ca. 190–210°C).

Haake Torque Rheological Measurement
The melt processing of PFSI precursors is further simulated with Haake torque rheological measurement. The information about the melt processability, thermal stability, and even decomposition temperature for the analyzed polymer can be readily obtained from the variation of torque with processing time at different temperatures. As depicted in Figure 5(a) is the plot of mixing torque of IEC0.92 melt against mixing time at 200–220, and 240°C, respectively. In general, IEC0.92 melt exhibits very low mixing torque. And the mixing torque increases significantly with mixing time before reaching a local maximum, decreases at a slower rate and levels off in the end. Meanwhile, the mixing torque decreases dramatically with melt temperature. With the increasing of melt temperature, the mixing equilibrium (constant mixing torque) is achieved at shorter mixing time and lower mixing torque. For instance, the leveled-off torque is 5.1 and 2.1 Nm for the IEC0.92 melt at 200 and 220°C, respectively. The torque decreases further to 0 Nm for the melt at 240°C. It is should be noted that small bubbles can be observed from the melt mixing at 240°C, probably due to the decomposition of low molecular weight polymer under shearing force at high temperature.

According to the capillary rheological measurement, IEC0.97 melt possesses lower viscoscity than IEC0.92 at the same temperature [Figure 5(b)]. Since the torque of IEC0.92 at 200–240°C is quite low, the torque rheological measurement for IEC0.97 was conducted at 10°C lower melt temperatures

(ca. 190, 210, and 230°C, respectively). Similar to IEC0.92, the leveled-off torque of 5.3, 2.4, and 0 Nm is observed for IEC0.97 melt at 190, 210, and 230°C, respectively. Small bubbles, due to decomposition of polymer chains were observed from melt mixing at 230°C.

By comparing the results from both TGA and torque rheological measurement, one may found that the thermal stability of PFSI precursors decreases at dynamical heating condition, where the heating is accompanied with shear and/or stretch. And, the thermal stability decreases with the content of –SO2F containing side-chains. For melt-extrusion of precursor membranes, the processed polymer should have relatively low melt viscosity, and low flowability is desired for film casting. A combined analysis of both MFI and torque testing, the processing temperature of PFSI precursors is found to be quite narrow. The processing temperature is thus suggested to be 225–235°C for IEC0.92, 215–225°C for IEC0.97, and 185–195°C for IEC1.05.

PFSI Membrane Structure Characterization
By using the optimized processing temperature for the PFSI precursors, PFSI membranes were prepared accordingly (Scheme 2). The PFSI precursor membranes were further base-hydrolyzed and acid-hydrothermal treated to prepare the membranes in acid form (PFSI-H). The conversion of –SO2F to –SO3H groups in PFSI side-chains can be easily characterized with IR spectra. Attenuated total reflection (ATR) data obtained for the precursor (IEC0.97) and acid form of PFSI are shown in Figure 6. The spectra were labeled with the aid of reference spectrum of Nafion®.[27] PFSI-H membrane was obtained by base-hydrolysis of IEC0.97 in 20% NaOH for 24 h and further acid conversion. The single IR band at 983.6 cm^{-1} is visible in both membranes, which is attributed to the symmetric stretching frequency of the ether (–COC–) next to the backbone[28] or to the CF stretching of the CF2–CF(CF3)–group of the side chain.[29]

In comparison, the characteristic peaks at 1468 and 822.3 cm^{-1}, assigned for –SO2F groups, disappear completely in the converted PFSI-H membrane. A new IR band appears at 1061.57 cm^{-1}, which agrees well with the characteristic peak for –SO3$^-$. This absorbance further confirms the conversion of –SO2F
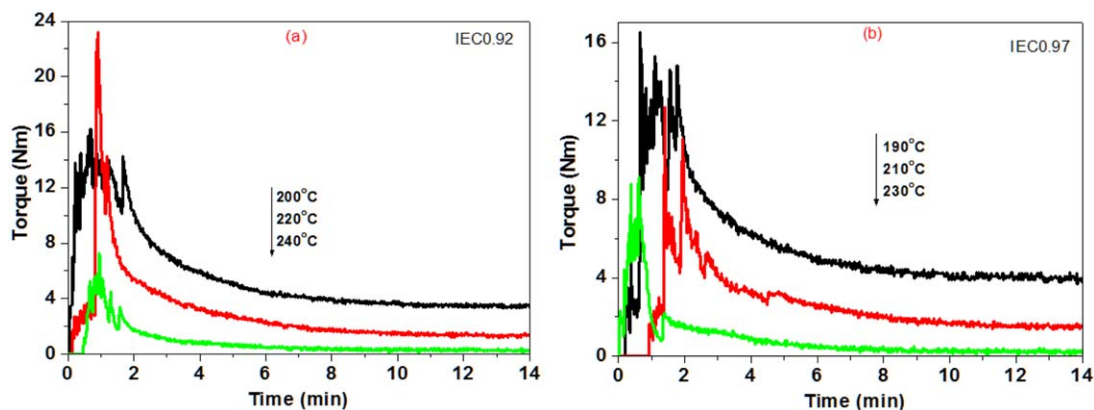

Figure 5. Plot of torque versus kneading time for (a) IEC0.92 resin at 200–240°C and (b) IEC0.97 resin at 190–230°C. [Color figure can be viewed in the online issue, which is available at wileyonlinelibrary.com.]
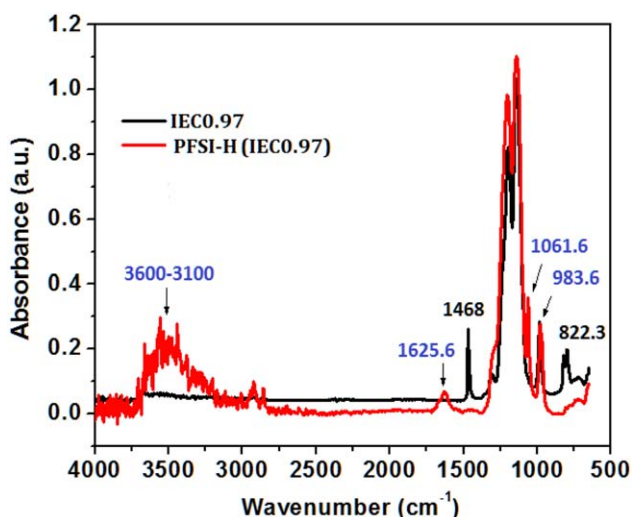
Figure 6. ATR-IR spectra of IEC0.97 and PFSI-H membranes, showing the characteristic peaks of the precursor and hydrogen bonding in PFSI-H membrane. [Color figure can be viewed in the online issue, which is available at wileyonlinelibrary.com.]

group into $-SO_3^-$ groups, endowing the membrane with ion-exchange capability. The remarkable IR band for PFSI membranes is observed at 3100–3600 cm^{-1}, which agrees well with the characteristic peak for intermolecular hydrogen bonding. This strong broad peak further shows the existence of $-SO_3H$ groups. The strong intramolecular hydrogen bonding may be beneficial for enhancing mechanical properties for the as-prepared PFSI-H membranes.

Crystallinity of PFSI Membrane

The introduction of polar $-SO_3H$ group in side-chain brings strong ionic interactions among PFSI polymer chains. These interactions are part of reasons why PFSI in both salt form and acid form cannot be extruded for fabrication.[2] As discussed above, PFSI-H possesses strong intramolecular hydrogen bonding and intermolecular ionic interactions in polymer chains. These interactions will greatly impede the packing of polymer chains into ordered crystalline structure. Hence, the PFSI-H membranes exhibit decreased crystallinity. Figure 7 compares a typical XRD spectrum of IEC0.92 and its converted PFSI-H membrane, together with PFSI-H membrane from IEC0.97. In comparison to IEC0.92, the corresponding PFSI-H membrane exhibits the same diffraction profile but decreased intensity in diffraction maximum and much right-tilted peak profile. The FWHM of PFSI membrane increased from 2.47 (IEC0.92) to 4.17 (PFSI-H) after conversion of IEC0.92 into acid form. According to the deconvultion of XRD peak for polyfluorocarbon backbone, the right-tilted peak shape indicates an increased portion of amorphous phase for polyfluorocarbon backbone in PFSI-H membrane.

A comparison of PFSI-H membranes with different ion-exchange $-SO_3H$ groups indicates that crystallinity decreases with IEC, mainly due to the strong ionic interactions among the polymer chains. The reduction in crystallinity between precursor and its corresponding PHSI-H membrane is larger for high IEC membranes.

Mechanical Properties of PFSI-H Membranes

The complete conversion of $-SO_2F$ group into SO_3Na is crucial to achieve good PFSI membranes for various applications. Hence, the effect of base-hydrolysis on the tensile properties of the resulted membranes was investigated. IEC0.97 membranes (0.25 mm in thickness) were base-hydrolyzed in 20% NaOH at 80°C for certain time and acid-hydrothermal for 24 h to ensure complete conversion of sodium into proton. Figure 8(a) shows the stress–strain curves of IEC0.97 and its base-hydrolyzed membranes with different duration. Typical ductile plastic fracture behavior with a tensile strength increasing with strain is observed for all curves. The stress–strain curve with unclear yielding transition was also observed for the as-received Nafion® membranes.[3] However, the elongation of base-hydrolysis time for IEC0.97 membrane significantly changes the nature of the curves. With increasing base-hydrolysis time, the tensile strength of PFSI membranes first increases dramatically within first 5 h and then levels off. The strain of PFSI membranes decreases by 50% over 3 h's base-hydrolysis and levels off afterwards [Figure 8(b)].

The 1 h base-hydrolyzed IEC0.97 membrane displays similar stress–strain curve as the precursor membrane, i.e., no obvious yielding is observed up to an elongation at break over 500% in the tensile testing. However, the breaking strength increases from 20.6 to 27.7 MPa, indicating 1 h base-hydrolysis initiated certain hydrolysis and hardening on the membrane surfaces. The base hydrolysis could gradually complete over 5 h since the membrane obtains significant improvement in tensile strength (36.58 MPa). However, the elongation at break decreases to 180%. A tensile strength of 38.2 MPa is obtained after 24 h's base-hydrolysis, which is much higher than that of dry Nafion®112 membrane (23.5 MPa).[14] The increase in yield strength can be explained by electrostatic cross-linking and strain induced further crystallinity, due to the increased strong ionic strength in PFSI membranes.

In Figure 8(b), the elongation at break decreases from 185% to 148% when extending the hydrolysis time from 5 h to 24 h. For membrane after 24 h's base hydrolysis, a tensile necking behavior
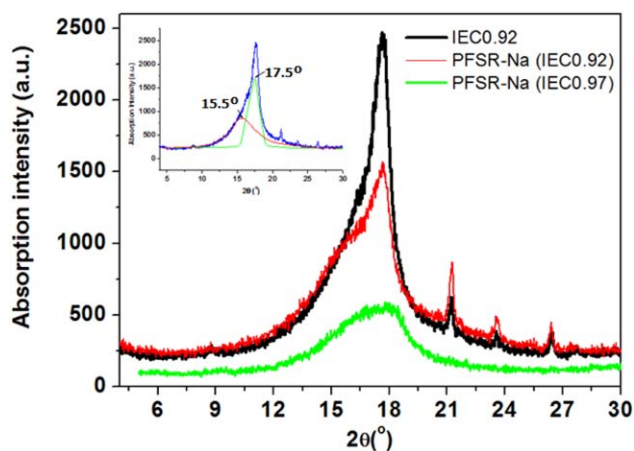

Figure 7. XRD curves of IEC0.92 and the acid form membranes for IEC0.92 and IEC0.97. Inset figure illustrates the deconvolution of the XRD curve of IEC0.92. [Color figure can be viewed in the online issue, which is available at wileyonlinelibrary.com.]
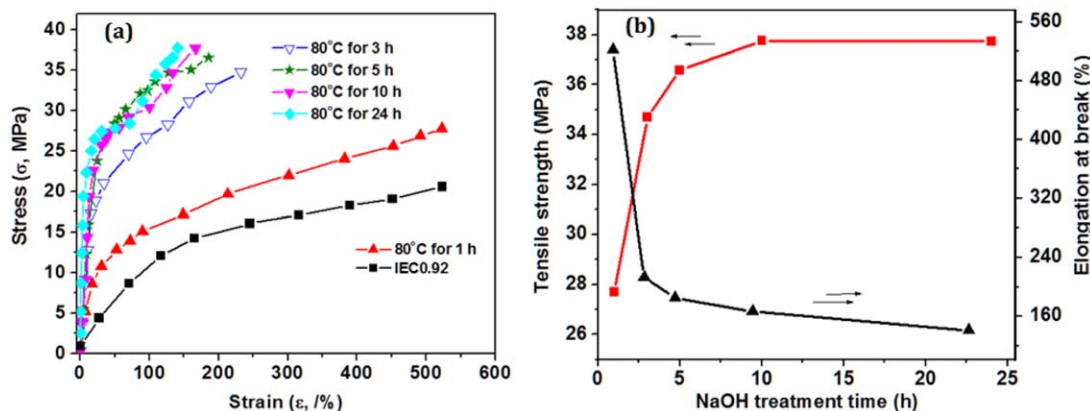
Figure 8. Stress–strain curves for IEC0.97 and its converted membranes with different duration of base-hydrolysis, (b) variation of tensile strength and elongation at break for PFSI-H membranes base-hydrolyzed in 20% NaOH at 80°C for different duration. [Color figure can be viewed in the online issue, which is available at wileyonlinelibrary.com.]

in cool stretching was observed. An obvious surface hardening was also observed for PFSI-H membranes after the complete conversion of the flexible precursor membranes. Enhanced glass transition temperature (T_g) was also found for the converted membranes in comparison to its precursor, meanwhile the semi-transparent precursor membranes changed into non-transparent after conversion. All these behaviors may be explained by the association of polymer chains, driven by the strong ionic interactions from the active in-exchange side-chains.

Water Uptake, Proton Conductivity, and Methanol Permeability of Membranes

High water uptake is a prerequisite for a good proton-exchange membrane because water would induce a dissociation of the protons from $-SO_3H$ groups and would also act as "vehicles" for the transportation of the protons from the anode to the cathode.[30] The water uptake of membranes was determined according to the procedure as in Ref. 14. The variation in water content of three PFSI-H membranes and reference Nafion 117
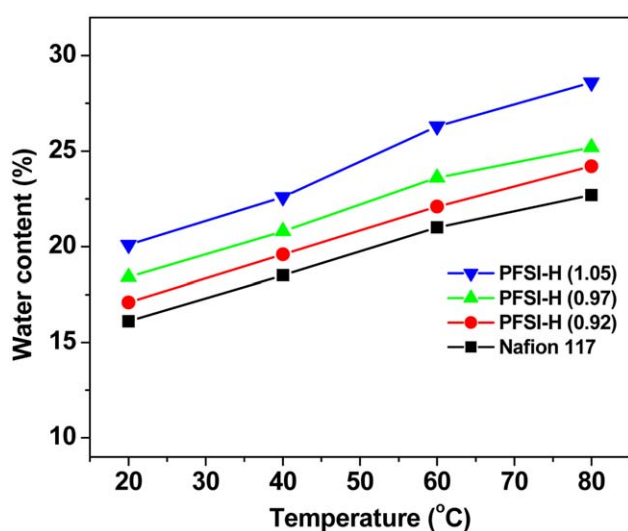
membrane with temperature is shown in Figure 9. Water content of all the membranes increased as the temperature increased. At the same temperature, water content of PFSI-H was larger than that of Nafion membranes. For PFSI-H membranes, the higher IEC value of the membrane, the bigger the water uptake. The higher water uptake for membranes with high IEC values is attributed to the enhanced hydrophilicity when increasing content of $-SO_2H$ containing side-chains to contribute higher IEC.

The proton conductivities of various membranes were also measured as in-plane values according to the procedure in Ref. 10. As compared in Table II, the proton conductivity of a PFSI-H (IEC = 0.92) membrane is about 12.1×10^{-3} S/cm, which is comparable to that of a Nafion117 membrane (11.5×10^{-3} S/cm) measured by using the same apparatus and testing conditions. The proton conductivity of the PFSI membranes gradually increases with the content of $-SO_2H$ containing side-chains, as indicated by the IEC values of PFSI-H membranes. As a result, the higher IEC value, the higher the proton conductivity of the membrane.

The methanol permeability of various membranes was also determined and the results are illustrated in Table II. It can be seen that the methanol permeability of PFSI-H membranes is slightly lower than that of the Nafion117 membrane. And the permeability decreases with IEC value of PFSI-H membrane. The slightly enhanced methanol crossover through the membranes can be attributed to the hydrophilic nature of $-SO_2H$

Figure 9. Temperature dependence of water uptake of PFSI-H and Nafion 117 membranes. [Color figure can be viewed in the online issue, which is available at wileyonlinelibrary.com.]

Table II. Proton Conductivity Values of Various Membranes

Membranes	Proton conductivity ($\times 10^{-3}$ S/cm)	Methanol permeability ($\times 10^{-7}$ cm^2/s)
PFSI-H (0.92)	12.1	3.98
PFSI-H (0.97)	12.8	3.80
PFSI-H (1.05)	13.6	3.76
Nafion 117	11.5	3.60

containing side-chains which increase the methanol solubility in higher IEC PFSI-H membranes.

CONCLUSION

Novel perfluorosulfonated ionomers membranes with different IEC values were successfully fabricated via melt-extruding and casting of the $-SO_2F$ precursors. The melt-processability of the precursors was evaluated through a systematical investigation of their thermal stability, crystallinity, and rheological properties. By extrusion-casting of precursor membranes, the acid form PFSI membranes were obtained with base-hydrolysis and acid-hydrothermal. The results show that the base-hydrolysis duration has a strong effect on the tensile properties of the as-prepared membranes. The content of $-SO_2F$ or $-SO_3H$ containing side-chains plays an important role in the thermal stability, rheological, and mechanical properties of the precursor of PFSI-H membranes. The strong ionic interactions attributed to the $-SO_3H$ groups lead to decreased crystallinity and tensile strength for different IEC PFSI membranes. The as-prepared PFSI membranes may have great potential for ion-exchange applications.

REFERENCES

1. Heitner-Wirguin, C. *J. Membr. Sci.* **1996**, *120*, 1.

2. Mauritz, K. A.; Moore, R. B. *Chem. Rev.* **2004**, *104*, 4535.

3. Slade, S.; Campbell, S. A.; Ralph, T. R.; Walsh, F. C. *J. Electrochem. Soc.* **2002**, *149*, A1556.

4. Saito, M.; Arimura, N.; Hayamizu, K.; Okada, T. *J. Phys. Chem. B* **2004**, *108*, 16064.

5. Ghielmi, A.; Vaccarono, P.; Troglia, C.; Arcella, V. *J. Power Sources* **2005**, *145*, 108.

6. Moore, R. B.; Martin, III C. R. *Anal. Chem.* **1986**, *58*, 2569.

7. Grot, W. G. European Patent 0,066,369 (**1982**).

8. Rhee, C. H.; Kim, H. K.; Chang, H.; Lee, J. S. *Chem. Mater.* **2005**, *17*, 1691.

9. Silva, R. F.; Passerini, S.; Pozio, A. *Electrochim. Acta* **2005**, *50*, 2639.

10. Luan, Y.; Zhang, H.; Zhang, Y.; Li, L.; Li, H.; Liu, Y. *J. Membr. Sci.* **2008**, *319*, 91.

11. Silva, R. F.; De Francesco, M.; Pozio, A. *Electrochim. Acta* **2001**, *49*, 3211.

12. Liu, C.; Martin, C. R. *J. Electrochem. Soc.* **1990**, *137*, 510.

13. Bahar, B.; Mallouk, R. S.; Hobson, A. R.; Kolde, J. A. US RE37, 307E (**2001**).

14. Liu, F.; Yi, B.; Xing, D.; Yu, J.; Zhang, H. *J. Membr. Sci.* **2003**, *212*, 213.

15. Spethmann, J. E.; Keating, J. T. US Pat. 6,110,333 (**2000**).

16. Satterfield, M. B.; Majsztrik, P. W.; Ota, H.; Benziger, J. B.; Bocarsly, A. B. *J. Polym. Sci. Part B: Polym. Phys.* **2006**, *44*, 2327.

17. Sauguet, L.; Ameduri, B.; Boutevin, B. *J. Polym. Sci. Part A: Polym. Chem.* **2007**, *45*, 1814.

18. Tang, W. H.; Zhu, T.; Zhou, P.; Zhao, W.; Wang, Q.; Feng, G.; Yuan, H. L. *J. Mater. Sci.* **2011**, *46*, 6656.

19. Tang, J.; Tang, W. H.; Yuan, H. L.; Jin, R. *J. Appl. Polym. Sci.* **2007**, *104*, 4001.

20. Tang, W. H.; Tang, J.; Yuan, H. L.; Jin, R. *J. Appl. Polym. Sci.* **2011**, *122*, 461.

21. Tang, W. H.; Tang, J.; Yuan, H. L.; Jin, R. *J. Polym. Sci. Part B: Polym. Phys.* **2007**, *45*, 2136.

22. Moore, R. B.; Martin, III C. R. *Macromolecules* **1988**, *21*, 1334.

23. Fujimura, M.; Hashimoto, T.; Kawai, H. *Macromolecules* **1981**, *14*, 1309.

24. Tadmor, Z.; Gogos, C. G. Principles of Polymer Processing; Wiley: New York, **2006**.

25. Tang, J.; Tang, W. H.; Yuan, H. L.; Jin, R. *J. Appl. Polym. Sci.* **2010**, *115*, 190.

26. Scott, G. W.; Blair, J.; Hening, C.; Wagstaff, A. *J. Phys. Chem.* **1939**, *43*, 853.

27. James, P. J.; Antognozzi, M.; Tamayo, J.; McMaster, T. J.; Newton, J. M.; Miles, M. J. *Langmuir* **2001**, *17*, 349.

28. Cable, K. M.; Mauritz, K. A.; Moore, R. B. *J. Polym. Sci. Part B: Polym. Phys.* **1995**, *33*, 1065.

29. Liang, Z.; Chen, W.; Liu, J.; Wang, S.; Zhou, Z.; Li, W.; Sun, G.; Xin, Q. *J. Membr. Sci.* **2004**, *233*, 39.

30. Kreuer, K.-D. *Chem. Mater.* **1996**, *8*, 610.